AN ULTRASONIC IMAGING SYSTEM FOR THREE-DIMENSIONAL HIGH-RESOLUTION DEFECT IMAGING

K. Mayer, R. Marklein, K.J. Langenberg, and T. Kreutter

Dept. Electrical Engineering
University of Kassel
Wilhelmshoherallee 71
D-3500 Kassel, FRG

INTRODUCTION

Quantitative ultrasonic imaging requires algorithmic data processing to yield the object function of a penetrable scatterer or the singular function of a perfectly scattering geometry, respectively. If either broadband pulse-echo or pitch-catch data are available on a closed measurement surface surrounding the scatterer completely, it can be shown that diffraction tomographic data processing in the widest sense is a solution of the linearized inverse scattering problem, i.e., if either the Born or Kirchhoff approximation can be tolerated in the NDE application under concern[1,2]. A particular representative of diffraction tomography called FT-SAFT for Fourier Transform Synthetic Aperture Focusing Technique has been implemented on an array processor for 3D defect imaging utilizing complementary Golay sequences[8] as transmitted signals to improve the signal-to-noise ratio and therefore, via deconvolution, the axial resolution. Data acquisition, storage, processing and sophisticated graphics display is controlled by an IBM-PC. In [3] the system as well as its theoretical background is described in detail, hence, only a brief and qualitative account is given here.

QUANTITATIVE ULTRASONIC IMAGING

Ultrasonic defect imaging in solids requires the solution of the full elastodynamic inverse scattering problem, which is rather complicated, and, hence, certain solutions have only been reported recently[4,5]. Figure 1 illustrates the problem that has to be solved. Elastic waves are excited within a test specimen applying a volume force density f to its surface; wave propagation is then governed by the equation

$$(\lambda + 2\mu)\nabla\nabla \cdot \mathbf{u} - \mu\nabla \times \nabla \times \mathbf{u} - \varrho\frac{\partial^2 \mathbf{u}}{\partial t^2} = -\mathbf{f} \qquad (1)$$

where u is the displacement vector in the homogeneous isotropic attenuation-free and frequency independent bulk material with Lame constants λ and μ and density ρ. Applying a Fourier transform with respect to the time variable t - ω denotes the corresponding frequency - we obtain a solution of Equation 1 in terms of a volume integral over the volume force density, which represents the incident field from the transducer, and a surface integral extending over the surface S_c of the scattering defect (compare Fig. 1)[6]. This solution is most appropriate for inverse scattering purposes, because the scattered field as the quantity to be measured on the surface of the test specimen is given by

Review of Progress in Quantitative Nondestructive Evaluation, Vol. 9
Edited by D.O. Thompson and D.E. Chimenti
Plenum Press, New York, 1990

the surface integral which contains the displacement on the surface S_c as well as the normal component of the stress tensor $T \cdot n$ as field dependent equivalent sources on S_c characterizing the defect. Hence, we "simply" have to invert this integral representation, i.e., we somehow have to invert the elastic wave propagation in terms of the second and third rank Green's tensors G and Σ, respectively, which account for the "transfer" of the equivalent sources on S_c - indicated by the circle in Fig. 1 - to the displacement field on the specimen surface - indicated by the dot. Algorithms achieving this goal have been proposed in [4,5]; unfortunately, apart from being rather complex, they rely on simultaneous measurements of both normal and tangential displacement components on the measurement surface, which, with present day ultrasonic equipment, is not yet easily possible. Therefore, we introduce a simplification of the problem, which is addressed by the keyword "scalarization"; the essential features are discussed along with Fig. 2. We decompose the displacement vector into a scalar and a vector potential, i.e., into pressure (P) and shear (S) waves. Then, the scalar potential Φ satisfies a scalar wave equation, which exhibits the "scalarized transducer" as inhomogeneity q_P. Once again, a Huygens type solution is appropriate for inverse scattering, but this time, the P-wave propagation from the defect surface to the measurement surface is governed by a scalar Green's function, G, and the field dependent equivalent sources on S_c are simply given by the scalar potential itself as well as its normal derivative. These sources can be roughly interpreted describing a P-defect, i.e., the defect as it is "seen" in the pressure wave mode when illuminated by a pressure wave. In the context of full elastodynamic inverse scattering (compare [4]) a thorough meaning can be given to this interpretation; similarly, S-wave incidence and observation of the mode converted fields can be "scalarized".

Again, our task is now the inversion of the surface integral of Fig. 2, when $\Phi(R,\omega)$ on the measurement surface is considered to be the data. To do this, further specification of the equivalent sources is appropriate. For the three canonical cases of penetrable scatterers - modeling solid inclusions in a solid -, and perfect scatterers with either a soft or a rigid boundary condition - modeling voids or perfect inclusions in a solid - equivalent volume sources q_c can be defined as follows - k_p is the pressure wave number

$$\begin{aligned} q_c^{pen} &= -k_P^2 O(\mathbf{R})\Phi(\mathbf{R},\omega) \\ q_c^{soft} &= -\gamma(\mathbf{R})\mathbf{n}\cdot\nabla\Phi(\mathbf{R},\omega) \\ q_c^{rigid} &= -\Phi(\mathbf{R},\omega)\nabla\cdot\gamma(\mathbf{R})\mathbf{n} \end{aligned} \qquad (2)$$

$$(\lambda+2\mu)\nabla\nabla\cdot\mathbf{u} - \mu\nabla\times\nabla\times\mathbf{u} - \varrho\frac{\partial^2\mathbf{u}}{\partial t^2} = -\mathbf{f}$$

$$\mathbf{u}(\mathbf{R},\omega) = \iiint_V \mathbf{f}\cdot\mathbf{G}\,dV + \iint_{S_c}[\mathbf{u}\cdot(\mathbf{n}\cdot\Sigma) - (\mathbf{T}\cdot\mathbf{n})\cdot\mathbf{G}]\,dS$$

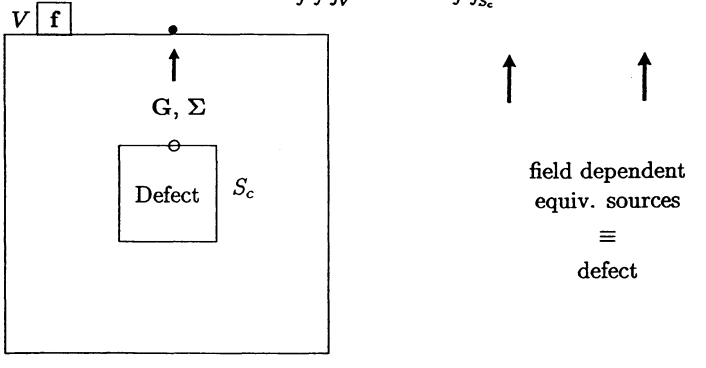

Figure 1 Elastodynamic inverse scattering problem.

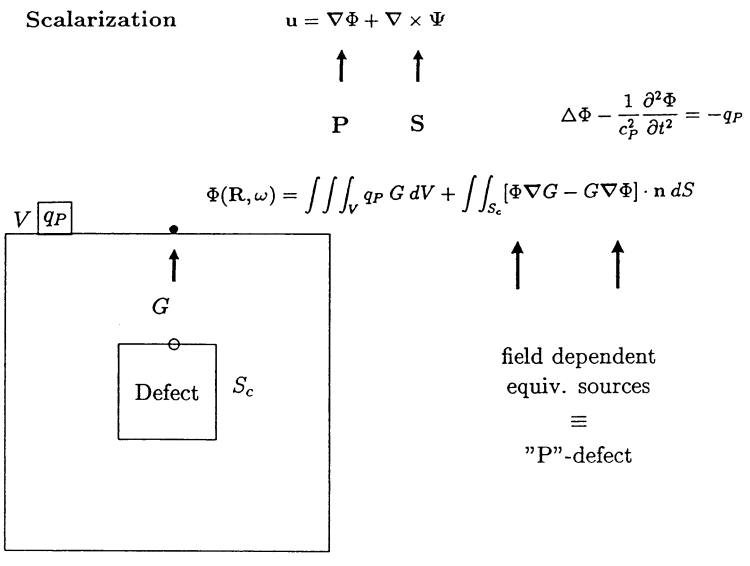

Figure 2 Scalarization of the inverse scattering problem.

where the object function O (R) is roughly proportional to the scattering volume V_c, and the singular function $\gamma(R)$ characterizes the surface S_c. Then, the surface integral

$$\iint_{S_c} [\Phi\nabla G - G\nabla\Phi]\cdot \mathbf{n}\, dS \tag{3}$$

can be transformed into a volume integral [2]

$$\iiint_{V_c} q_c G\, dV \tag{4}$$

and, hence, the inverse scattering solutions are formally independent of the particular scatterer under concern. Additionally, we recognize that the equivalent volume sources are always dependent upon the total field on or in the scatterer, which requires the introduction of a further approximation to be discussed below. First, we introduce the backpropagation argument as the keyword of imaging (compare Fig. 3). Considering the scattered potential on the measurement surface S_m - denoted by $\overset{M}{\Phi}_s$ - as formal equivalent sources on S_M, we can define a field quantity Θ_H in the vicinity and on the scattering surface via backpropagation of Φ_s^M (and $\nabla\Phi_s^M \cdot n$ utilizing a complex conjugate Green's function G* within a Huygens type surface integral extending over S_M; Θ_H is called the generalized holographic field [1], which can be transformed into a volume integral representation involving the above defined equivalent volume sources and the imaginary part G; of Green's function. This representation of the generalized holographic field relates a field quantity, which can be deduced from measurements and a source quantity describing the defect; it is called Porter-Bojarski integral equation [1] and serves as starting point for the evaluation of a unified theory of linearized scalar inverse scattering [1,2]. Linearization has to be introduced in the following sense

$$q_c \simeq \Phi_i \tag{5}$$

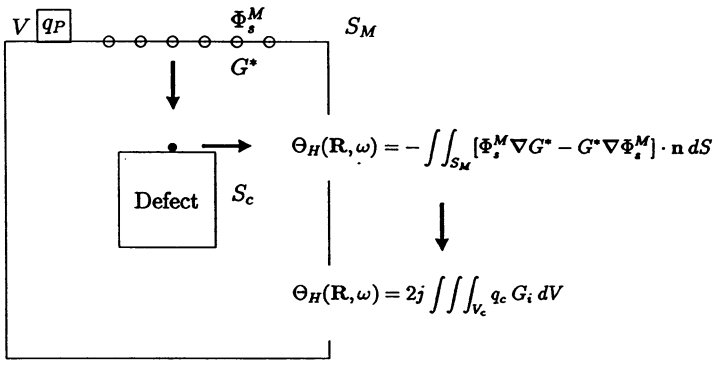

Figure 3 Inverse scattering via backpropagation.

i.e. replacing the total field appearing in the equivalent volume sources by the incident field alone. For the penetrable scatterer, this approximation is known as weak scatterer or Born approximation, and for the perfect scatterer it is associated with the physical optics argument and the name of Kirchhoff. Only within these approximations, the Porter-Bojarski integral equation can be integrated with respect to frequency or with respect to the angle of illumination, computational steps, which are necessary for its inversion. If these approximations can be tolerated in practical NDT applications, a variety of imaging algorithms can be deduced within this framework starting with conventional holography and ending up with the formerly heuristic SAFT-algorithm, which has therefore found a thorough theoretical basis now. For planar measurement surfaces it turns out that the Porter-Bojarski integral equation reduces to the well-known Fourier Diffraction Sice Theorem [7,1], and, hence, the time domain backpropagation scheme SAFT has an algorithmic counterpart, which uses Fourier transforms only. To emphasize the relationship of this processing alternative with SAFT we have chosen the name FT-SAFT. It is essentially the algorithm, which has been implemented in its pulse-echo version in our three-dimensional ultrasonic imaging system.

Since our theory of ultrasonic imaging contains X-ray Computer Tomography as well as Diffraction Tomography as special cases we call it a general diffraction tomographic theory of inverse scattering. It is a quantitative theory in the sense that it yields a well defined output under well defined approximations. Especially, the output consists of

- The object function for the penetrable scatterer
- That part of the scattering surface, which is "visible" from the measurement surface for the perfect scatterer

if the following assumptions and approximations are satisfied or can be tolerated [3]

- scalarization
- linearization (Born, Kirchhoff)
- infinite bandwidth
- infinitely large planar or arbitrarily closed aperture

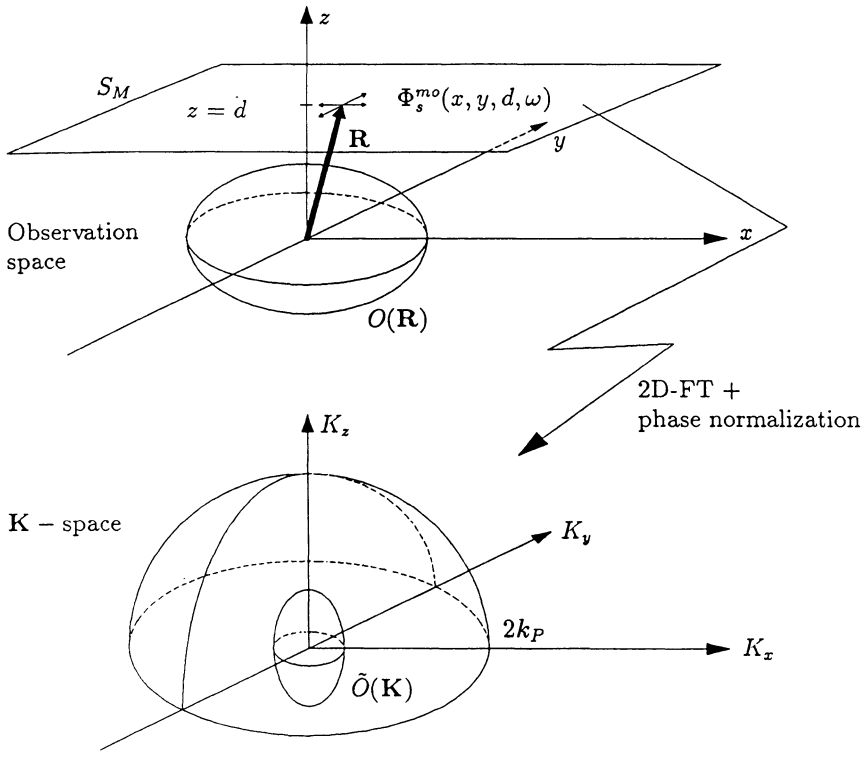

Figure 4 Pulse-echo FT-SAFT.

- point source transducer in the pulse-echo experiment or plane wave excitation in the pitch-catch experiment
- homogeneous isotropic attenuation free and frequency independent bulk material

Most often, assumptions like infinite bandwidth and infinite aperture are not realized; in that case, at least the resulting image degradation can be calculated quantitatively.

THREE-DIMENSIONAL IMAGING WITH FT-SAFT

The algorithmic processing of time domain SAFT data via Fourier transforms is explained in Figure 4. The corresponding mathematics are given in [3]. A planar measurement surface S_M resides at the plane z = d of a cartesian coordinate system, x, y, z; the defect is characterized by its object function O(R). Time domain data of the scattered field are taken on S_M and transformed into the frequency domain; for the pulse-echo case, some modification of the data is required [3] resulting in $\Phi_s^{mo}(x,y,d,\omega)$. A further two-dimensional Fourier transform with respect to the aperture variables x and y together with a phase normalization allows the mapping of the transformed data onto a sphere with radius $2k_P$ in the spatial Fourier space (K-space) of the defect, thus giving access to the three-dimensional Fourier transform $\tilde{O}(K)$ of the object function. A final three-dimensional inverse Fourier transform results in the object function itself, or for the case of a perfect scatterer, in that part of the singular function, which is "visible" from S_M.

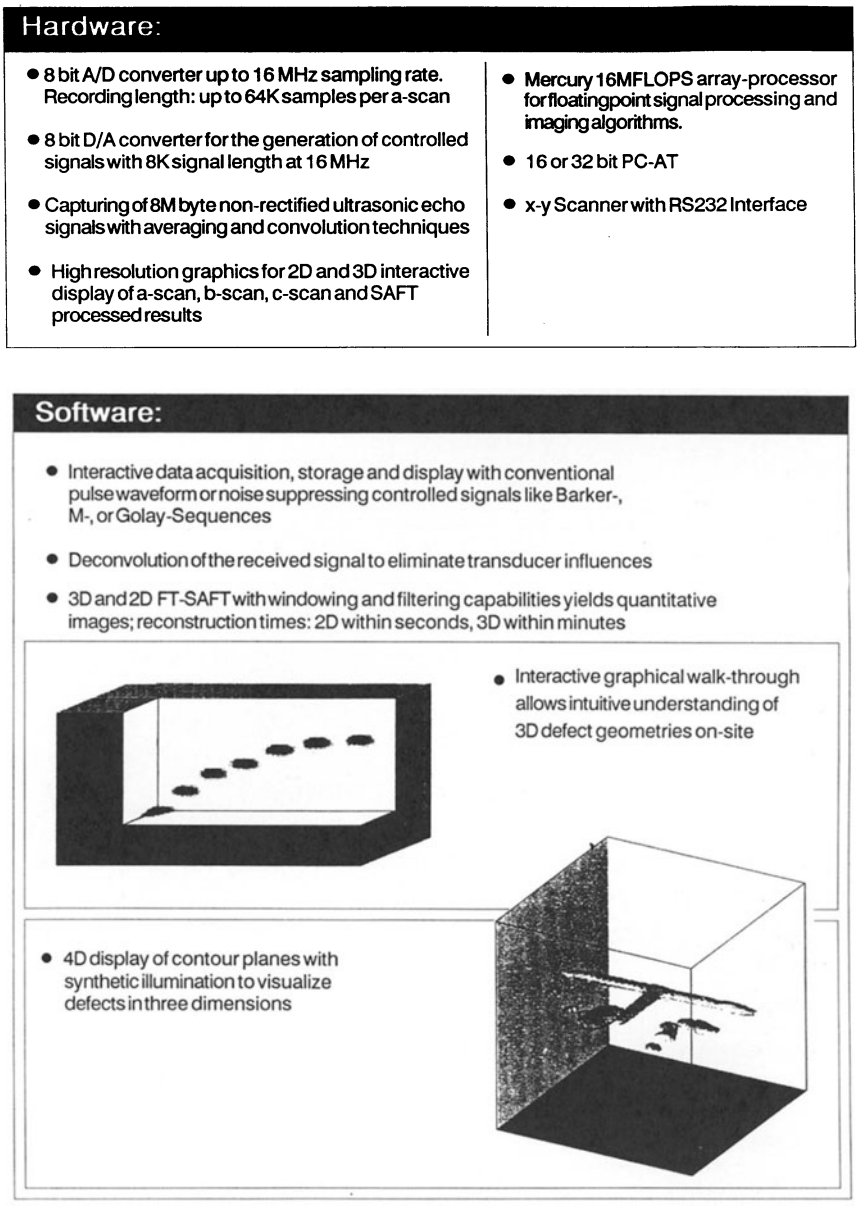

Figure 5 Necessary hardware and available software of the three-dimensional ultrasonic imaging system.

HIGH RESOLUTION IMAGING VIA COMPLEMENTARY GOLAY-SEQUENCES

As mentioned earlier, the input of FT-SAFT requires infinite transducer bandwidth to yield a sharp imaging of, for instance, the singular function, i.e. the scattering surface. At least in principle, this bandwidth can be recovered from real life experiments via

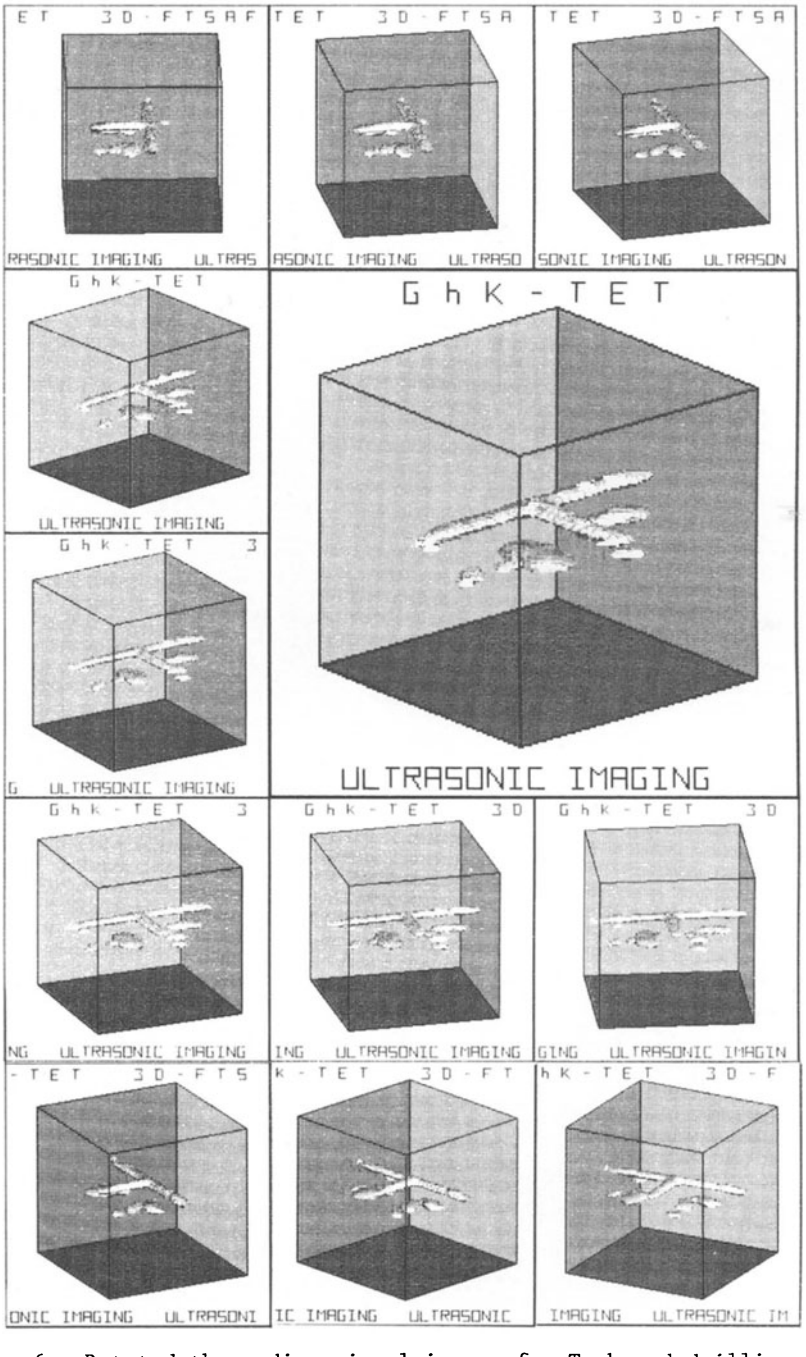

Figure 6 Rotated three-dimensional image of a T-shaped drilling in a solid with nearby crack-fields.

deconvolution. Practical limitations are imposed by the available signal-to-noise ratio. Therefore, in the imaging system to which we refer in this paper, special care is taken to improve the signal-to-noise ratio in order to be able to apply spectral deconvolution subsequently. A detailed investigation of a variety of available sophisticated input signals has shown, that so-called complementary Golay-sequences [8] exhibit the best performance in the context of the imaging system. Two N-bit sequences are transmitted at each aperture point, which are complementary in the sense, that the sum of their autocorrelation functions is given by a delta-function of amplitude 2N. The received signals are correlated with their pertinent transmitted signals, added and deconvolved within the usable bandwidth with similarly obtained reference signals, for example via the backwall of the specimen. The result is the bandlimited impulse response of the scatterer, which serves as input into FT-SAFT. All necessary computational operations - Golay-sequence selection, correlation, deconvolution, Fourier transforms - are performed on an array processor being controlled by an IBM-PC.

ULTRASONIC SYSTEM FOR THREE-DIMENSIONAL HIGH-RESOLUTION DEFECT IMAGING

Besides a scanner and an ultrasonic unit the system comprises a PC, an array processor and a high-resolution graphics screen. The necessary hardware and the available software is listed in Fig. 5. More specific information can be found in [3], especially with regard to the number of time and aperture samples to be processed into a certain number of volume pixels, i.e., voxels. Typically, 64 x 64 x 64 voxels are obtained within minutes. In [3] applications of the system to various different NDT problems are discussed, and selected modes of 3D data display are reported. In Fig. 5 two representatives are referenced; first, a possible walk-through along three orthogonal planes of the 3D data field is indicated for a particular test specimen, and second, a 4D contour plot of a certain iso-surface of the three-dimensional image is given for a real life application, i.e. a T-shaped drilling in a solid being used for high-pressure liquid flow, whence crack fields are observed nearby. The latter image representation can be calculated for a variety of different look angles, in fact, 22 can be stored on the graphics board under concern. These 22 views can be subsequently projected into the center of the screen in order to produce a real time rotation of the three-dimensional defect image. Fig. 6 gives an impression of what is visible on the screen; the remaining views reside in the virtual memory of the board.

REFERENCES

1. G. T. Herman, H. K. Tuy, K. J. Langenberg, P. Sabatier: Basic Methods of Tomography and Inverse Problems, Adam Hilger, Techno House, Bristol, 1987.
2. K. J. Langenberg: Introduction to the Special Issue on Inverse Problems. Wave Motion 11 (1989) 99-112.
3. K. Mayer, R. Marklein, K. J. Langenberg, T. Kreutter: A 3D Ultrasonic Imaging System Based on FT-SAFT. Ultrasonics (1989) (to appear).
4. K. J. Langenberg, T. Kreutter, K. Mayer, P. Fellinger: Inverse Problems and Imaging. Conf. Proc. of the International Union of Theoretical and Applied Mechanics (Ed: S.K. Datta), Boulder, 1989.
5. A. T. Devaney: Elastic Wave Inverse Scattering and Diffraction Tomography. Conf. Proc. of the International Union of Theoretical and Applied Mechanics (Ed: S. K. Datta), Boulder, 1989.
6. Y.-H. Pao, V. Varatharajulu: Huygens' Principle, Radiation Conditions, and Integral Formulas for the Scattering of Elastic Waves. J. Acoust. Soc. Am. 59 (1976), 1361-1371.
7. A. C. Kak, M. Slaney: Principles of Computerized Tomography, IEEE Press, New York, 1988.
8. M. J. E. Golay: Complementary Series, IRE Trans. Info. Theory IT-7 (1961) 82.